RERTR 2010 _ 32ND INTERNATIONAL MEETING ON
REDUCED ENRICHMENT FOR RESEARCH AND TEST REACTORS
October 10-14, 2010
Lisboa Hotel
Lisbon, Portugal

RESULTS OF SEM AND TEM CHARACTERIZATION OF A DISPERSION FUEL PLATE WITH AL-2SI MATRIX TESTED IN THE RERTR-7 EXPERIMENT

D. D. KEISER, JR., J. F. JUE, J. GAN, A. B. ROBINSON, P. MEDVEDEV, B. MILLER, AND D. M. WACHS
Nuclear Fuels and Materials Division, Idaho National Laboratory
P. O. Box 1625, Idaho Falls, Idaho 83403 USA

ABSTRACT

As part of the RERTR fuel development program, U-7Mo dispersion fuel plates with different matrix Si contents have been irradiated under a variety of different irradiation conditions. In the RERTR-7 experiment, two fuel plates with 2 wt% Si added to the matrix (R2R040 and R2R050) were irradiated at fission rates that were higher than those for fuel plates irradiated in the RERTR-6 experiment. The microstructure of the fuel plate R2R040 has been recently characterized using scanning and transmission electron microscopy. SEM characterization was performed on a sample taken from the low and high flux side of the fuel plate and TEM analysis was performed on a sample taken from the high flux side. It was observed that significant Si penetration from the fuel/matrix interaction (FMI) layer into the U-7Mo fuel had occurred during irradiation. This penetration was much more dramatic compared to what had been observed for a fuel plate with 2 wt% Si in the matrix (R2R010) irradiated as part of the RERTR-6 experiment. The presence of Si in the U-7Mo fuel appeared to impact the growth of fission gas bubbles during irradiation. Areas of Si-depletion were observed in the FMI layers.

1. Introduction

The United States Reduced Enrichment for Research and Test Reactors (RERTR) Fuel development program is actively developing low enriched uranium (LEU) fuels for the world's research reactors that are currently fueled by uranium enriched to more than 20% ^{235}U [1].

To assess the performance of U-Mo dispersion fuels with Si-doped matrices, different reactor experiments have been conducted using the Advanced Test Reactor (ATR). For the purpose of conducting scanning electron microscopy examinations on irradiated samples, the RERTR-6 experiment has been of particular interest since the experiment was extracted from ATR over three years ago, and as a result, small samples can be handled in the Electron Microscopy Laboratory (EML). This paper will discuss the first microstructural characterization results from a more recently irradiated RERTR-7 U-7Mo dispersion fuel plate using a scanning electron microscope (SEM). Results from transmission electron microscopy (TEM) characterization of a high-flux sample from the fuel plate will also be discussed. The fuel plate that was characterized had Al-2Si alloy matrix. A low-flux sample taken from this fuel plate had already been characterized using transmission electron microscopy [2]. Optical metallography (OM) data will also be included. Focus will be given to the partitioning behavior of Si amongst the microstructural phases and how the presence of Si affects the development of fuel matrix interaction (FMI) layers at the U-7Mo/matrix interface. Comparisons are made to the other

irradiation experiments that have been reported for fuel plates with U-7Mo fuel dispersed in Al-2Si matrix.

2. Experimental

2.1 Irradiation Testing

The RERTR-7 experiment was conducted to test 6 gU/cc U-Mo dispersion fuels with Si-containing matrix to reactor conditions that were more aggressive than those tested in the RERTR-6 experiment. To achieve these conditions, the RERTR-7 experiment used enriched uranium (58.2% U-235) to control the power density of the fuel [3], which produced higher fission rates in the different fuel plates compared to the RERTR-6 plates. The average burnups were between 50 and 90% LEU equivalent at the end of irradiation. The fuel plates were positioned edge-on to the core, and as a result had a neutron flux gradient across the widths of the fuel plates.

This paper focuses on the U-7Mo dispersion fuel plates with Al-2Si matrix that were tested in the RERTR-7A part of the experiment, which came out of the reactor in March of 2006 after 90 effective full power days of irradiation. The irradiation conditions for the two characterized fuel plates with Al-2Si matrix are enumerated in Table 1, along with the conditions for the RERTR-6 fuel plates with Al-2Si matrix that were characterized previously [4]. One RERTR-7 fuel plate (R2R050) was characterized using only OM and the other (R2R040) was characterized using OM and SEM. R2R040A is a punching taken from the low flux side of the fuel plate that was used for SEM, and R2R040B was taken from the high flux side and used for SEM analysis. R2R050A and R2R050B identify the irradiation conditions at locations where punchings would have been taken if similar SEM analysis had been conducted on that fuel plate.

Table 1. Irradiation conditions for U-7Mo/Al-2Si dispersion fuel plates containing U-7Mo atomized particles irradiated as part of RERTR-6 and RERTR-7 experiments.

Fuel Plate Label	Experiment	Peak Temp.(˚C)	Ave. Fission Density (10^{21} f/cm^3)	Ave. Fission Rate (10^{14} f/cm^{3}s)	Peak Heat Flux (W/cm^2)
R2R010A	RERTR-6	94	2.4	2.0	98
R2R010B	RERTR-6	109	4.5	3.8	148
R2R020	RERTR-6	104	3.1	2.7	139
R2R040A	RERTR-7	95	3.5	4.6	195
R2R040B	RERTR-7	122	6.3	8.1	340
R2R050A	RERTR-7	112	3.5	4.6	190
R2R050B	RERTR-7	135	5.8	7.5	310

2.2 Microstructural Characterization

For as-irradiated fuel plates, OM is performed on a transverse cross section taken from the mid-plane. SEM analysis is performed on a longitudinal cross section of a one-mm-diameter punching that is taken at either the low or high flux sides of the fuel plate. SEM analysis, with energy and wavelength dispersive spectroscopy (EDS/WDS), is performed on the mounted samples to characterize the microstructure and to determine the partitioning behavior, during irradiation, of different fuel and matrix components between the different fuel meat phases. TEM characterization is performed using a sample generated from a fuel punching that is similar to those used for SEM analysis.

3. Results and Discussion

3.1 Optical Metallography

For fuel plates R2R040 and R2R050, an OM image of a full transverse cross section taken at the mid-plane of the as-irradiated microstructure, along with higher magnification images at the low and high flux side of each fuel plate, are presented in Figs. 1 and 2, respectively. The microstructures in these OM images at the low and high-flux sides of the fuel plates do not necessarily coincide with the exact locations where a punching sample would be taken for SEM analysis. Fuel plate R2R050 contained more fuel/matrix interaction (FMI) layer than did R2R040. Based on Table 1, the thicker FMI layers are most likely due to the exposure of R2R050 to higher temperatures at the low and high flux sides of the fuel plate.

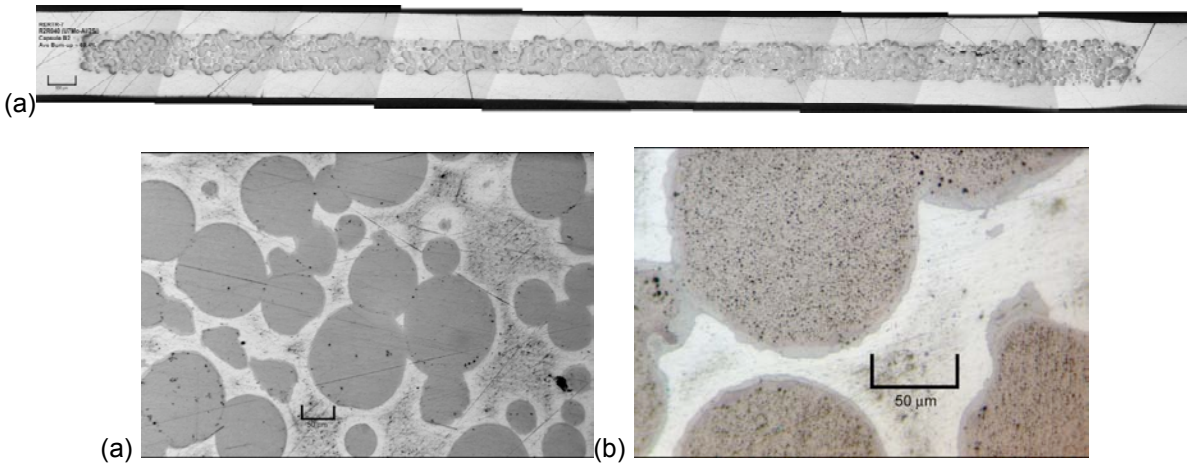

Fig. 1. A low-magnification optical micrograph (a) of the R2R040 fuel microstructure and higher magnification images at the (b) low and (c) high flux side of the fuel plate. The dark phase is U-7Mo alloy, the medium-contrast phase is FMI layer, and the bright phase is Al-2Si alloy.

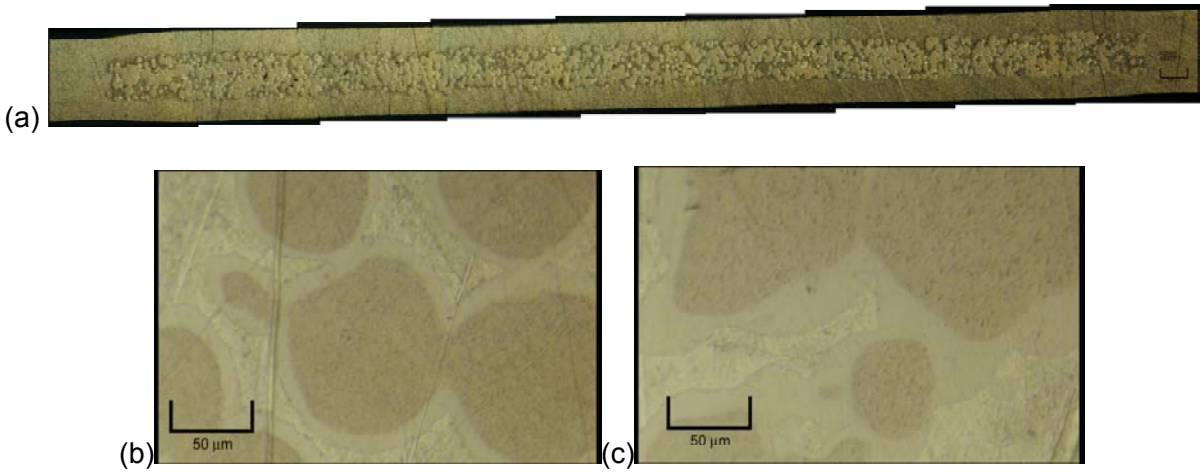

Fig. 2. A low-magnification optical micrograph (a) of the R2R050 fuel microstructure and higher magnification images at the (b) low and (c) high flux side of the fuel plate. The dark phase is U-7Mo alloy, the medium-contrast phase is FMI layer, and the bright phase is Al-2Si alloy.

3.2 Scanning Electron Microscopy
3.2.1 FMI Layers

SEM images of the microstructure observed for a sample produced at the low flux side of fuel plate R2R040 are presented in Fig. 3. Like was the case for the OM images (see Fig. 1), the FMI layer was observed to be a few microns thick and was not uniform. Low and high magnification X-ray maps for U, Mo, Al, and Si are presented in Figures 2 and 3, respectively. The relatively high Si concentrations observed on the U-7Mo alloy side of the FMI layer appears to be due to diffusion of Si from the FMI layer into the U-7Mo fuel during irradiation. It has been demonstrated that after fabrication there is a Si-rich FMI layer already present in U-7Mo dispersion fuel plates with Al-2Si matrix [5], and apparently during irradiation the Si diffuses from this layer into the fuel particles. Based on the Al X-ray maps in Figs 4 and 5, negligible Al diffuses into the fuel. Si enrichment has also been observed at the interface between the FMI layer and the Al-2Si matrix. This could be due to the fact that as the FMI layer grows into the Al-2Si matrix, the recoil zone that penetrates around 10 μm in front of the layer will extend further and further into the matrix, which results in interdiffusion of more Si towards the FMI layer, and this results in an enrichment of Si at the interface.

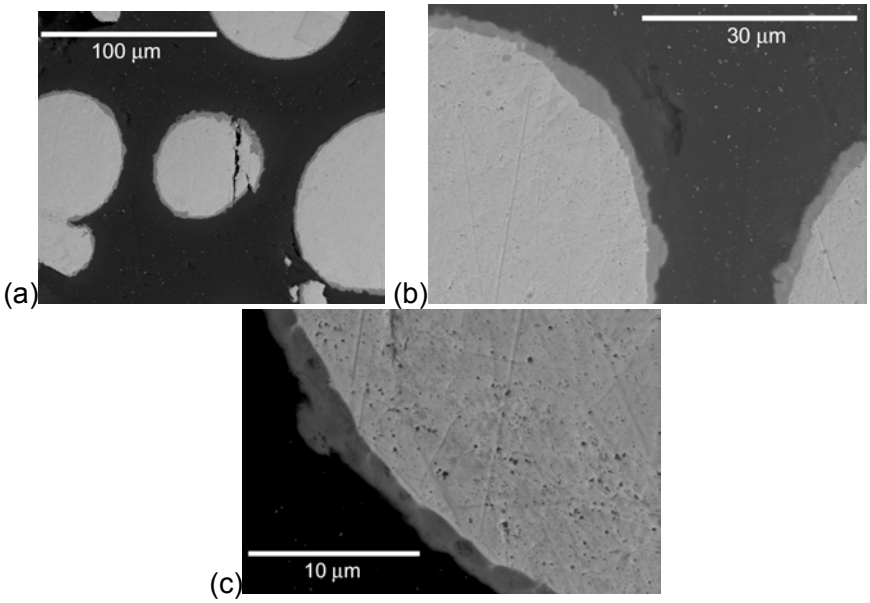

Fig. 3. Backscattered electron images (a-c) of the low flux side of the R2R040 fuel microstructure.

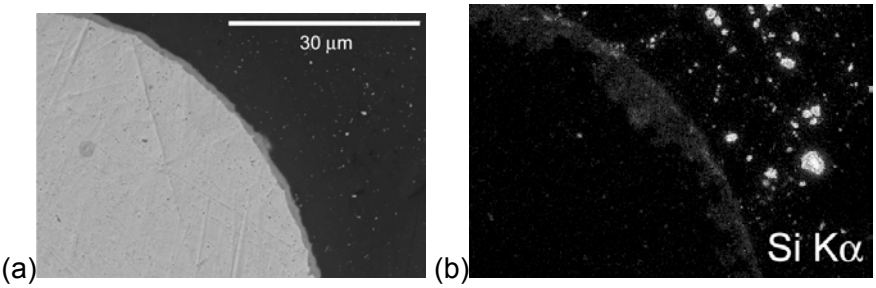

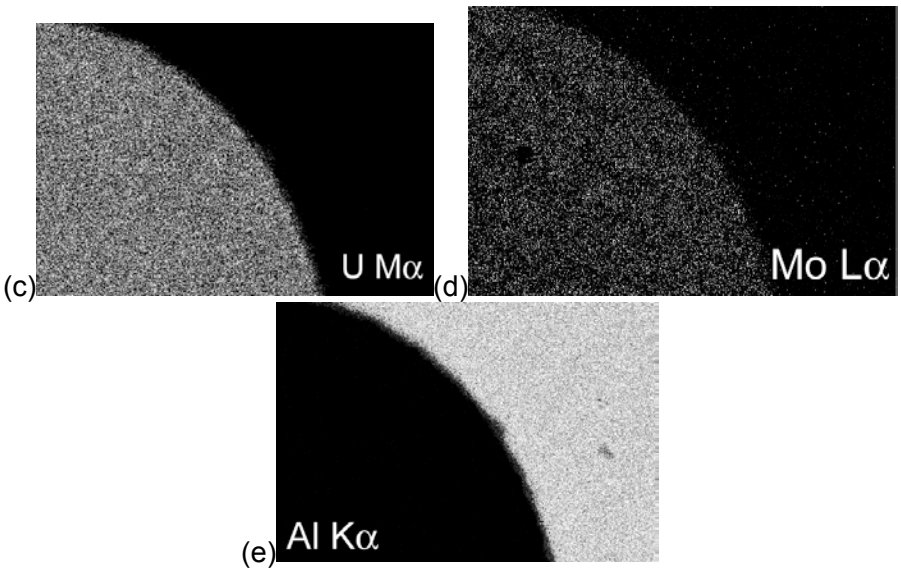

(c) (d) (e)

Fig. 4. Backscattered electron image (a) and X-ray maps for (b) Si, (c) U, (d) Mo, and (e) Al.

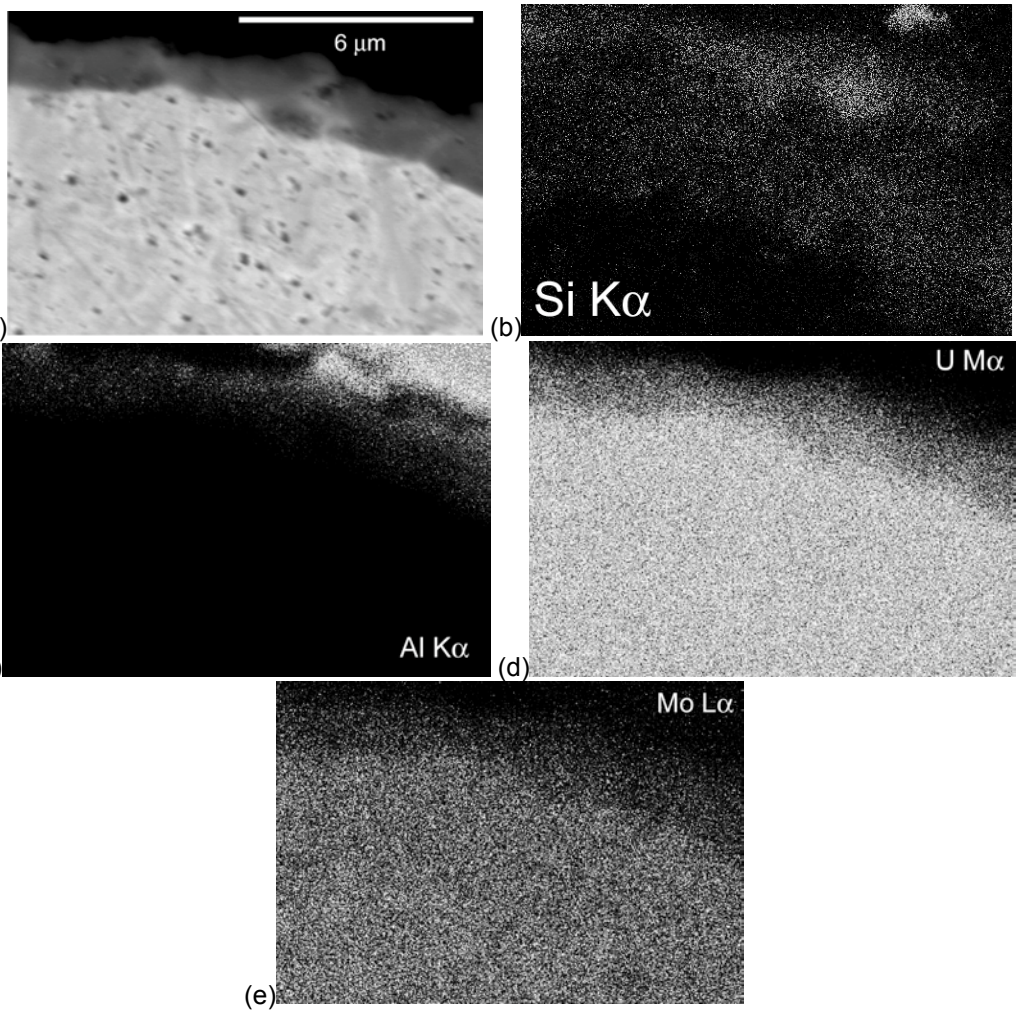

(a) (b) (c) (d) (e)

Fig. 5. Backscattered electron image (a) and X-ray maps for (b) Si, (c) U, (d) Mo, and (e) Al.

For the punching from the high flux side of the fuel plate, SEM micrographs of the microstructure are presented in Fig. 6. As was the case for the low-flux sample, FMI layers can be observed around the U-7Mo fuel particles that are not uniform. X-ray maps for U, Mo, Al, and Si are presented in Fig. 7, and a similar high concentration of Si is observed on the U-7Mo alloy side of the FMI layer, suggesting that Si diffused into the fuel during irradiation. The Si X-ray maps in Fig. 8 show that at the center of some FMI layers there is negligible Si and at the FMI layer/Al-2Si matrix interface there is again enrichment of Si. The Si X-ray maps in Fig. 9 show that some of the thickest FMI layers contain negligible Si. This may suggest that as the FMI layer grows during irradiation, and much of the original Si has already diffused into the fuel, there are local areas in the fuel meat matrix where there is not enough Si available for diffusion to occur into the FMI layer such that there will be significant Si in the layer.

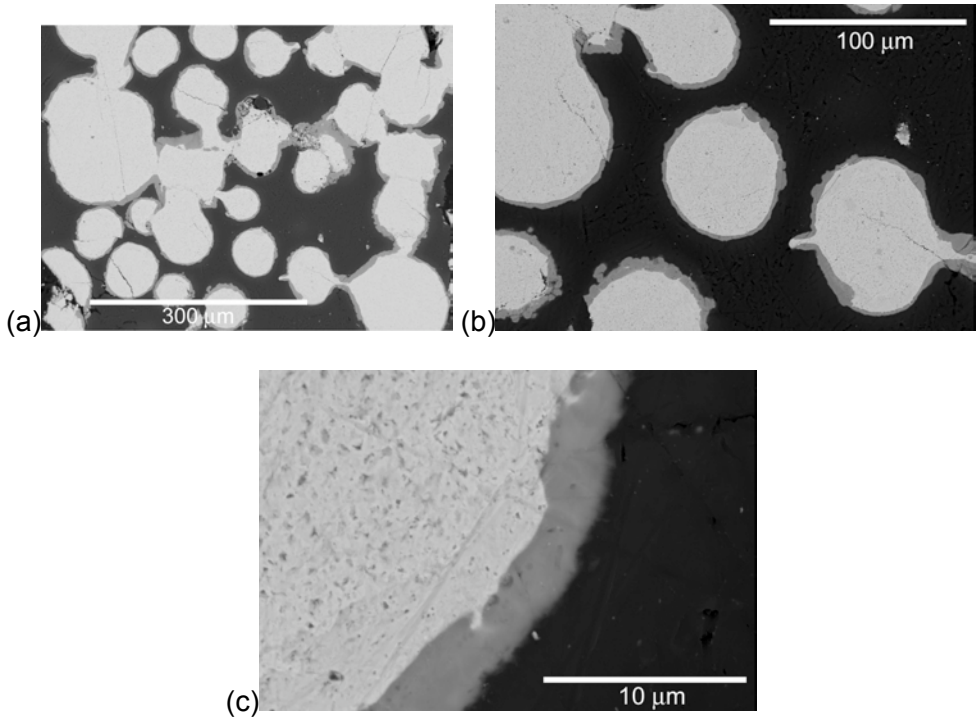

Fig. 6. Backscattered electron images (a-c) of the microstructure observed at the high flux side of the R2R040 fuel plate.

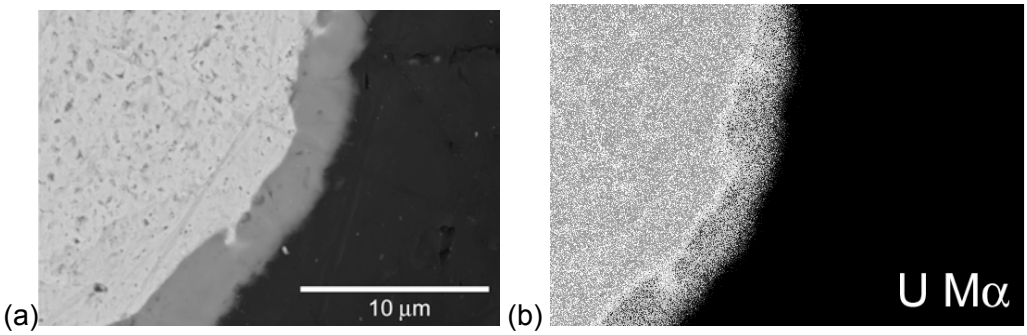

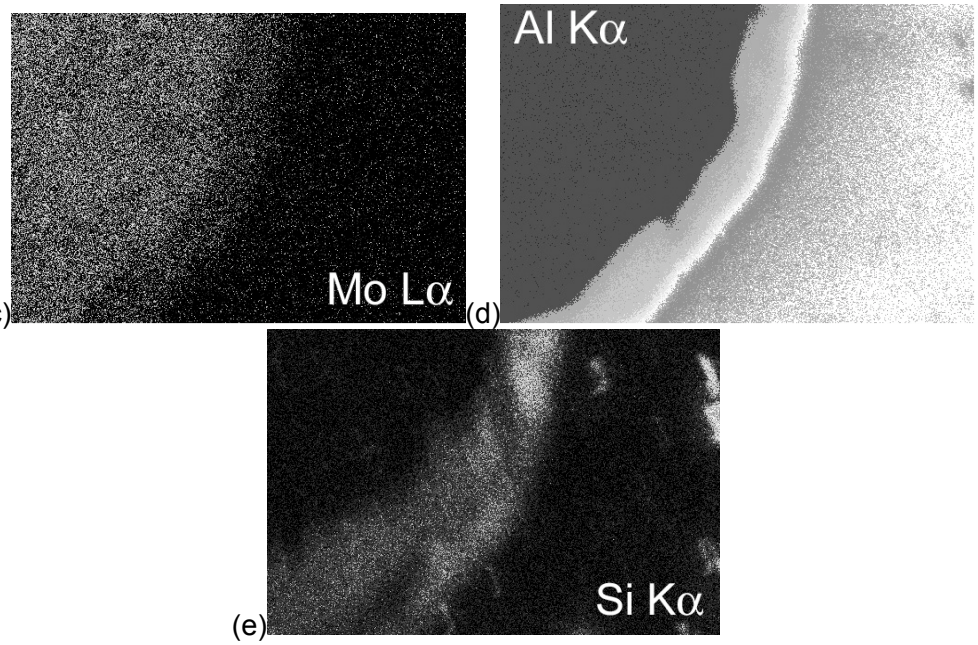

(c) (d) (e)

Fig. 7. Backscattered electron image (a) and X-ray maps for (b) U, (c) Mo, (d) Al, and (e) Si.

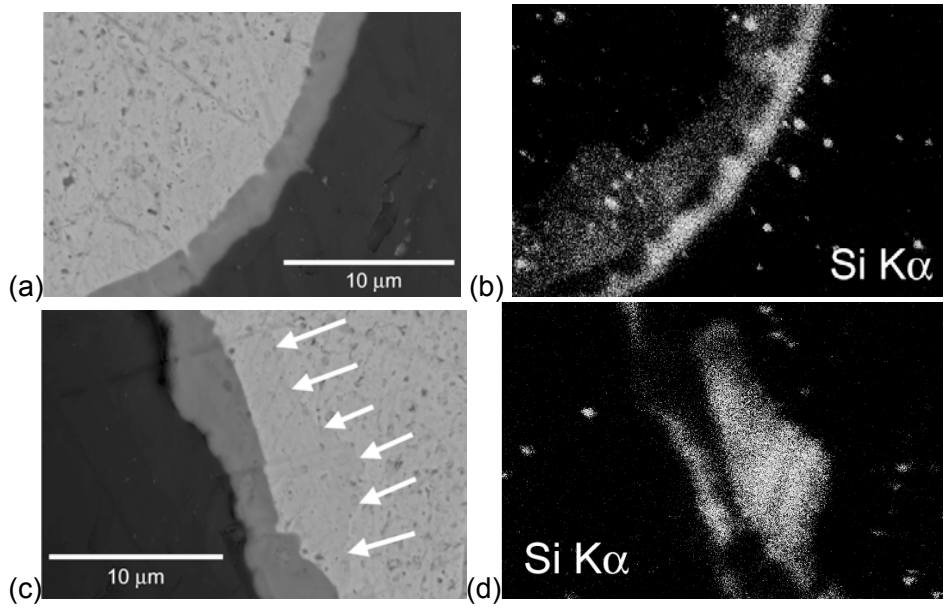

(a) (b) (c) (d)

Fig. 8. Backscattered electron images (a,c) and Si X-ray maps (b,d). The arrows in (c) identify the boundary that can identified where the Si-enrichment in the U-7Mo ends. The Si-rich precipitates in U-7Mo particle in (b) are most likely due to the Si impurity that has been observed in the U-7Mo particles in as-fabricated fuel plates.

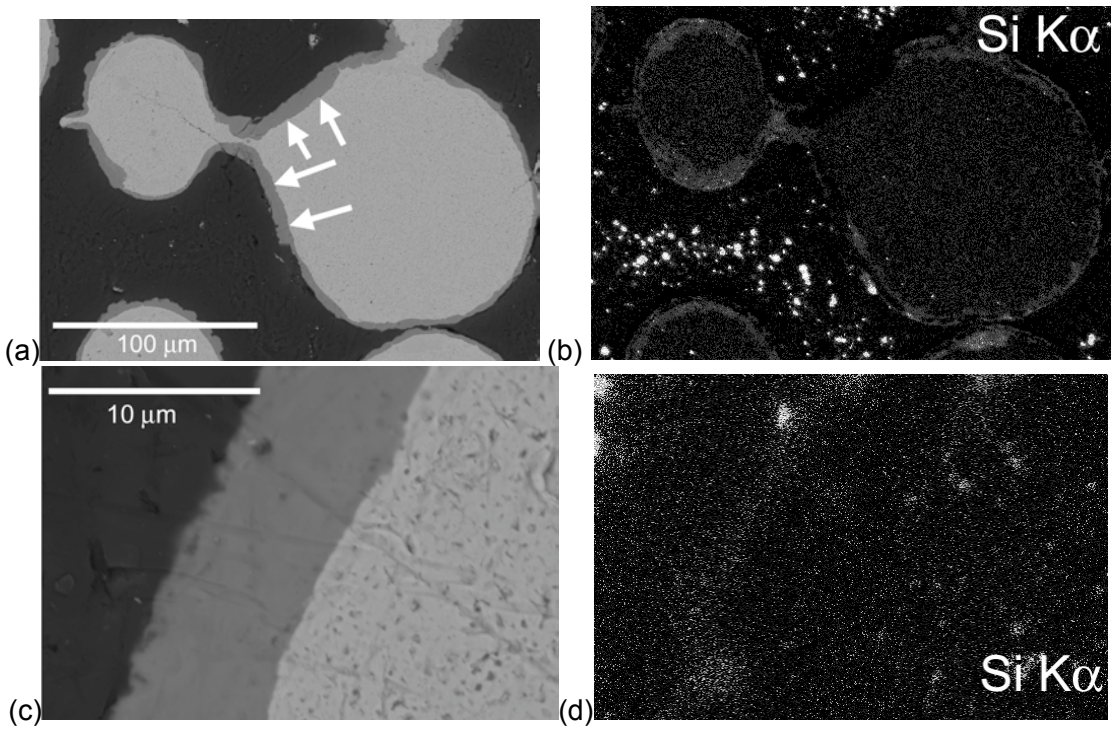

Fig. 9. Backscattered electron images (a,c) and Si X-ray map (b,d). The arrows in (a) show where there are relatively thick FMI layers that contain negligible Si. (c) Is a higher magnification image of a Si-deficient FMI layer.

Comparison of the results described above for the FMI layer growth behavior in the RERTR-7 U-7Mo dispersion fuel plates with Al-2Si matrix can be compared to those reported for other fuel dispersion fuel plates with Al-2Si matrix that were tested in other irradiation experiments and either SEM or EPMA analyses were performed. Qualifying fuel plates were irradiated in the RERTR-6 [4], IRIS-3 [6], IRIS-4 [7], IRIS-TUM [8], and KOMO-3 [9] experiments. However, the IRIS-4 fuel plates tested oxidized U-7Mo fuel particles, the IRIS-TUM experiment tested ground U-7Mo powders and the KOMO-3 experiment tested fuel pins, not plates, and as a result the most similar experiments for comparison are those from RERTR-6 and IRIS-3. As shown in Table 1, the RERTR-6 fuel plates were tested at lower temperatures, fission rates, and heat fluxes compared to the RERTR-7 fuel plates. As a result, the FMI layers did not experience as much growth during irradiation as did the RERTR-7 fuel plates, and not as much Si diffused from the FMI layers into the fuel. However, close examination of the generated results for the RERTR-6 samples does suggest that there was some migration of the Si from the FMI layers into the fuel. For the IRIS-3 fuel plate, which was irradiated to an average fission density of 3.4 x 10^{21} fcm^{-3} and an average fission rate of around 3.0 x 10^{14} $fcm^{-3}s^{-1}$, Si penetration from the FMI layers into the U-7Mo fuel was not reported. This could be due to the very low levels of FMI layer formation during fabrication, which would have been the source of the Si for penetration into the fuel. Some Si enrichment at the FMI layer/Al-2Si matrix interface of the fuel particles did seem apparent in the IRIS-3 plate, probably due to the Si diffusion towards the U-7Mo particles in the regions of the recoil zone.

3.2.2 Fission Gas Bubble Development

Fractured particles were present in both the low and high-flux samples that allowed for evaluation of the fission gas bubble distribution within the irradiated U-7Mo microstructure. SEM images of the observed fission gas bubbles in the U-7Mo microstructures for the low and

high-flux sample are presented in Figures 10 and 11, respectively. It can be seen that there is a significant difference in how the fission gas bubbles are distributed in the microstructures of the low and high flux samples. The low flux sample microstructure is comprised mainly of grains and grain boundaries with observable fission gas bubbles between the grains. However, the high-flux sample does not contain observable grains and the fission gas bubbles are unevenly distributed throughout the alloy. This difference in microstructure is probably due to the fact that at the irradiation conditions seen by the fuel in the high-flux sample, irradiation-induced recrystallization has occurred which can result in a dramatic change of the microstructure [10,11]. The low-flux sample appears to be just starting to recrystallize, which resulted in development of the small areas of fission gas bubbles between the U-7Mo grains.

The FMI layer did not exhibit the same fission gas bubble distribution as the U-7Mo fuel (see Fig. 12a and b). In addition, the fission gas bubble distribution was different in the areas of the U-7Mo that had become Si-enriched during irradiation (see Fig. 12c). TEM characterization results that have been reported for a punching sample from the low-flux side of the same fuel plate analyzed using SEM (R2R040) confirm this difference in fission gas bubble distribution [2]. This work demonstrated that the U-7Mo areas enriched in Si become amorphous during irradiation and therefore do not contain a fission gas superlattice, which directly impacts the fission gas bubble distribution in the material.

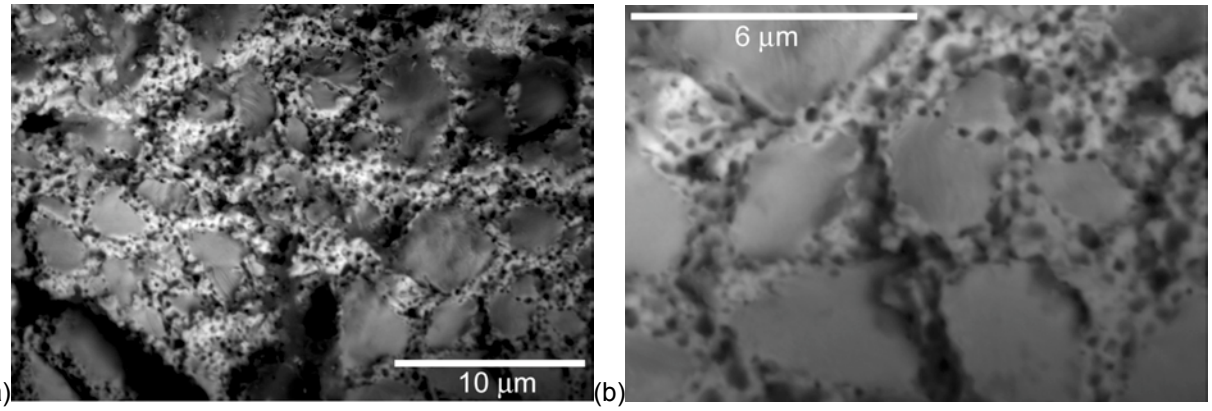

Fig. 10. Backscattered electron images (a,b) of fission gas bubbles in a U-7Mo particle in the low-flux sample.

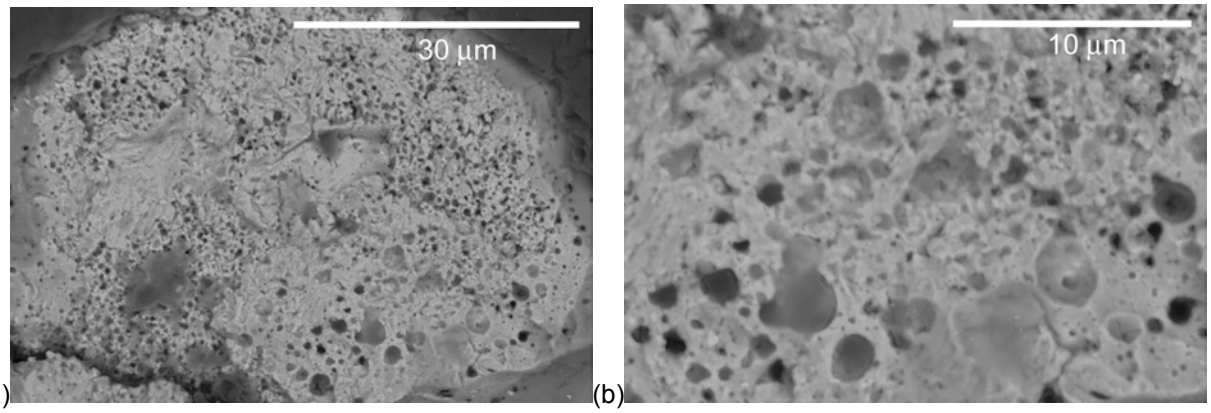

Fig. 11. Backscattered electron images (a,b) of fission gas bubbles in a U-7Mo particle in the high-flux sample.

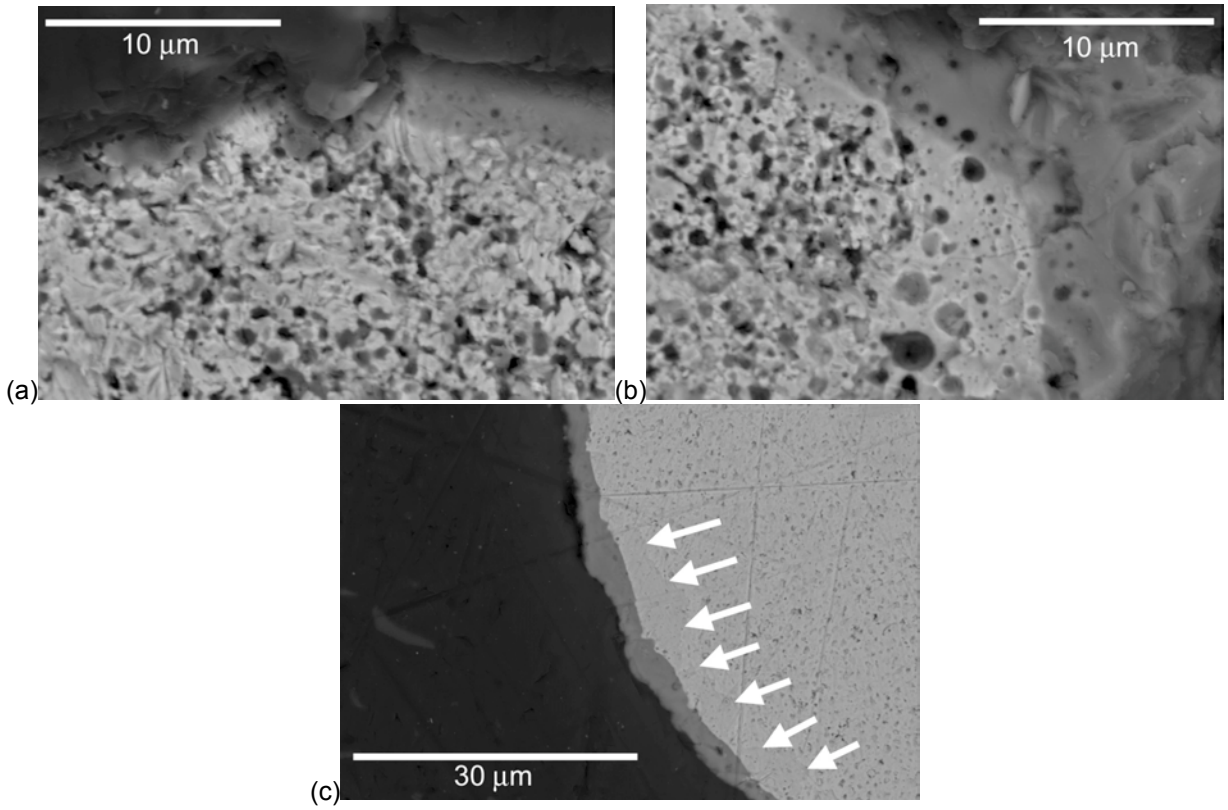

Fig. 12. Backscattered electron images (a,b) in a fractured U-7Mo fuel particle at the U-7Mo/FMI layer interface. The image in (c) is of a polished U-7Mo particle, and the arrows identify the boundary between an area of Si penetration into the U-7Mo and the fuel region where no Si could be observed. There seems to be a difference in the number of fission gas bubbles that can be resolved depending on whether or not there was Si penetration.

3.3 Transmission Electron Microscopy

TEM results have most recently been generated for a sample produced from the high-flux side of fuel plate R2R040. A comparison of low magnification (×2500) bright field images of the microstructure of a fuel particle from the high-flux sample is compared to a sample from the low-flux sample that was characterized earlier (see Figure 13 (a) and (b)). The increase in bubble density and size for the high flux condition is evident. Although a significant part of the fuel remains crystalline, many amorphous regions are identified. Areas surrounding the bubbles shown in light contrast are amorphous. Similar to the low flux condition, some of these irregularly-shaped bubbles are believed to be solid fission product precipitates. The residual superlattice of fine fission gas bubbles is observed in both amorphous and crystalline fuel regions as shown in high resolution images (× 50k) in Figure 13 (c) and (d). The presence of residual bubble superlattice in amorphous region of fuel suggests that the crystalline to amorphous transition, as a result of accumulated radiation damage, may occur before the bubble superlattice collapses from bubbles touching one another as their size increases.

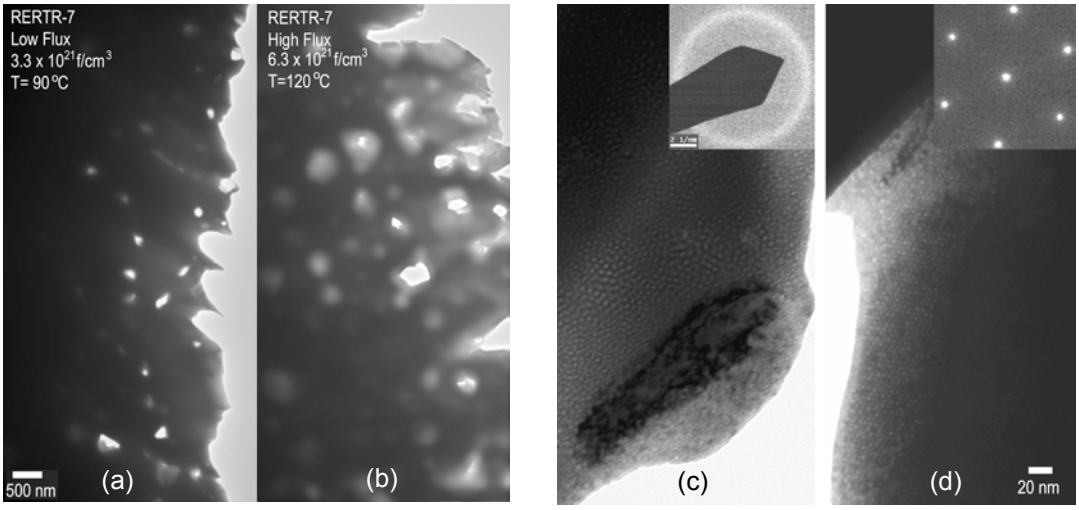

Figure 13. Comparison of low magnification views of a low (a) and high (b) flux particle showing an increase in bubble density and size for the latter. High resolution images are presented that show a residual bubble superlattice in amorphous (c) and crystalline (d) fuel.

Figure 14 shows the four-layer microstructure that was also found in the low flux condition. Note that the same correlation between Si content and the amorphous (high Si) and crystalline (low Si) fuel is observed for both low flux and high flux conditions. It seems that high Si in the U-7Mo fuel results in amorphization. Note that amorphous region in the high-flux sample has a Si content greater than ~ 4 at%, lower than that for the low-flux sample (Si > 10 at%). The corresponding composition measurements for the marked locations in Figure 14 are listed in Table 2. It appears that the FMI composition has a ratio of heavy element to light element (U+Mo)/(Al+Si) close to UAl_4. The low Si content (Si < 2 at%) for crystalline regions of fuel remains the same for both high flux and low flux conditions.

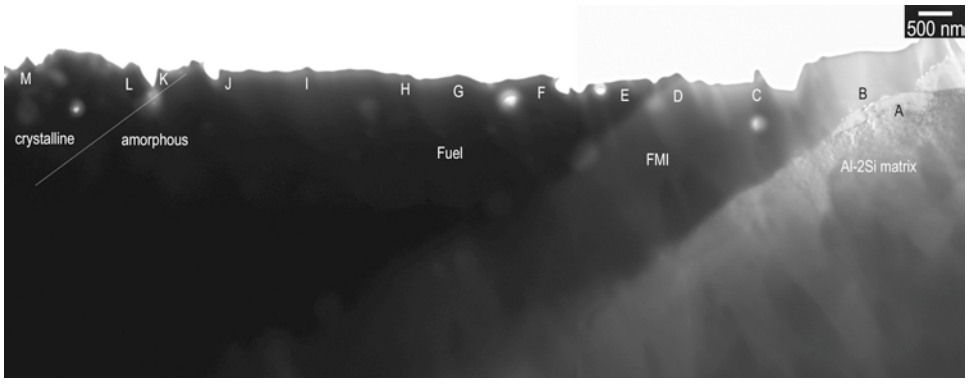

Figure 14. A TEM micrograph of the four-layer microstructure (crystalline fuel, amorphous rim of fuel, FMI and Al-2Si matrix) observed in the high-flux sample, which is similar to that at the low-flux condition. The letters mark the different locations where a composition measurement was made using energy-dispersive spectroscopy (EDS).

Table 2. EDS measurements (at.%) of the areas marked in Figure 14.

Spot	U	Si	Al	Mo	Note
A	0.5	2.4	96.0	1.1	Al-2Si matrix
B	10.2	11.2	74.4	4.3	FMI
C	12.9	4.0	79.2	3.9	FMI
D	15.2	3.8	76.1	4.8	FMI
E	34.3	16.8	38.4	10.5	Fuel, amorphous rim
F	47.3	11.8	28.3	12.6	Fuel, amorphous rim
G	48.7	12.0	25.7	13.6	Fuel, amorphous rim
H	49.6	12.5	23.3	14.6	Fuel, amorphous rim
I	41.3	19.8	26.3	12.6	Fuel, amorphous rim
J	53.9	9.8	20.5	15.8	Fuel, amorphous rim
K	59.0	1.9	25.4	13.7	Fuel, crystalline
L	60.0	0	23.0	17.0	Fuel, crystalline
M	62.9	0.6	17.8	18.7	Fuel, crystalline

Mo is one of the major fission products, and it is expected that the Mo content in the fuel or FMI will increase with burnup. A Mo-rich FMI layer has been observed near the fuel, as shown in Figure 15, that is amorphous. The EDS measurement shows a high Mo content up to 33 at% in these areas with typical values greater than approximately 20 at%. Most of these high-Mo FMI areas show much less bubbles than typical areas of FMI (Mo < 5 at%). The Mo-rich FMI often shows scattered micro-cracks, which will need to be investigated further to determine how they may impact fuel performance at very high burnup.

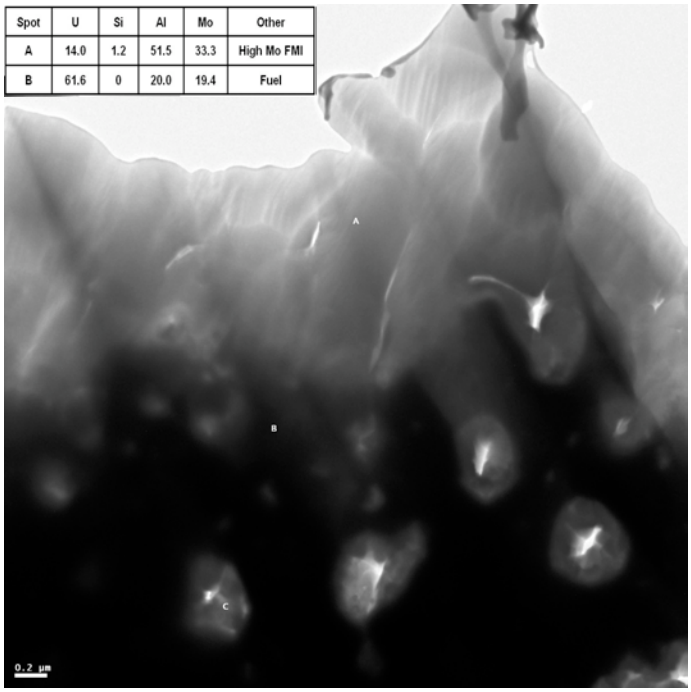

Figure 15. A TEM micrograph of a Mo-rich FMI layer, next to the fuel, with less or no large bubbles. Some micro-cracks can be observed.

Acknowledgments

This work was supported by the U.S. Department of Energy, Office of Nuclear Materials Threat Reduction (NA-212), National Nuclear Security Administration, under DOE-NE Idaho Operations Office Contract DE-AC07-05ID14517. Personnel in the Hot Fuel Examination Facility are recognized for their contributions in destructively examining fuel plates.

References

[1]. D. Wachs et al., Proc. of *GLOBAL 2007*, Boise, ID, September 9-13, 2007.
[2]. J. Gan et al., RRFM 2010, Marrakech, Morocco, March 21-25, 2010.
[3]. D. M. Wachs, et al., RERTR 2006, Cape Town, South Africa, Oct. 29-Nov.3, 2006.
[4]. D. D. Keiser, Jr. et al., RRFM 2009, Vienna, Austria, March 22-25, 2009.
[5]. D. D. Keiser, Jr. et al., RERTR 2008, Washington, D. C., October 5-9, 2008
[6]. A. Leenaers et al., RRFM 2008, Hamburg, Germany, March 2-5, 2008.
[7]. M. Ripert et al., RERTR 2009, Beijing, China, November 1-5, 2009.
[8]. W. Petry et al., RRFM 2008, Hamburg, Germany, March 2-5, 2008.
[9]. J. Park et al., RRFM 2008 Hamburg, Germany, March 2-5, 2008.
[10] G. L.Hofman and Y. S. Kim, Nucl. Engr. and Tech., 37 (2005) 299-308.
[11] Y. S. Kim et al., RERTR-2007, Prague, Czech Republic, Sep. 23-27, 2007.